CMOS Field-Modulated Color Sensor

Derek Ho, Glenn Gulak, and Roman Genov
Department of Electrical and Computer Engineering
University of Toronto

***Abstract*— A digital photosensor for multi-color imaging is presented. By modulating the electric field applied to the photo sensing region, the sensor reports light intensity at discrete wavelengths. It utilizes standard CMOS technology, integrating a spectrally-sensitive photodiode and a current-to-frequency analog-to-digital converter on the same die. A 0.35μm prototype demonstrates intensity measurement of 540nm (green) and 640nm (red) illumination with an optical sensitivity of 1μW/cm^2/level and consumes 0.3mW from a 3.3V supply.**

I. Introduction

Multi-color fluorescence imaging has become a popular way to discriminate between multiple proteins, organelles, or functions in a single or multi-cell organism [1]. This imaging technique is invaluable to many areas of the life sciences, in particular, to cancer research [2]. Multi-color fluorescence imaging utilizes biomarkers that absorb light and emit at longer and deterministic wavelengths, typically between 500nm to 700nm. Therefore, unlike other spectroscopic techniques, such as Raman spectroscopy, where continuous fine spectral resolution is required, fluorescent imaging requires spectral differentiation among several discrete wavelengths.

Conventionally, color separation has been achieved by using a set of optical bandpass filters to select different parts of the emission spectrum, as depicted in Fig. 1(a). The optics involved is bulky and expensive, and the mechanical swapping of filters prevents parallelization of this process. Methods based on diffraction grating (the splitting of light) [3] and Fabry-Perot etalon (tuned resonance cavity) [4] generally offer high spectral resolution, but require micromachining and post-processing such as wafer polishing and wafer bonding. Eliminating the need for sophisticated optics and post-processing is the ultimate remedy to high design complexity and fabrication cost.

Techniques that solely rely on integrated circuit process technology have been developed, most notably buried junction technology [5] (which the Foveon sensor is based on), as depicted in Fig. 1(b). Since light absorption in a semiconductor varies across wavelengths in such a way that light of a longer wavelength can penetrate deeper, a photocurrent measured at a deeper depth consists of stronger long-wavelength components. By sensing at several depths, color information can be inferred. Although the buried junction approach

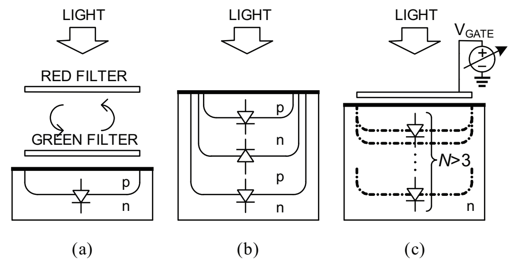

Fig. 1: Evolution of spectral imaging approaches. (a) Classical method of mechanically switching between optical filters. (b) Buried triple p-n-junction embedding diodes at three fixed depths. (c) Photo sensing region depth modulation enabling light collection at multiple electronically-tunable depths [6].

achieves high spatial density and is suitable for photographic applications requiring only three colors (e.g., red, green, and blue), there is a limit to the number of diodes that can be implemented, for example three for a dual-well process. This renders it unsuitable for applications that require sensing at many wavelengths.

To overcome this limitation, a spectrally-sensitive photodiode (SPD) that can sense more than three colors has been reported [6], [7]. A biased poly-silicon gate modulates the photo sensing region depth to effectively achieve an equivalent of many buried diodes ($N>3$), as depicted in Fig. 1(c). The most recently reported prototype is fabricated in a 5μm custom process [7].

In this paper, we present experimental results from a field-modulated color sensor (FCS) inspired by [6], [7] but prototyped in a standard digital 0.35μm CMOS technology, with on-chip analog-to-digital conversion, and digital readout circuits. This improves detection accuracy, minimizes power, and eliminates off-chip components. The FCS is scalable to an arrayed implementation, enabling color imaging.

II. Custom-CMOS Field-Modulated Color Sensors

When a semiconductor is illuminated, photons are absorbed and electron-hole pairs are generated. When an electric field is present, the photo-induced electrons can be collected to form a current [8]. The resulting photocurrent is given by

$$I = \frac{\phi q S \lambda}{hc}(1 - e^{-\alpha\omega}) \tag{1}$$

978-1-4577-0223-5/11/$26.00 ©2011 IEEE

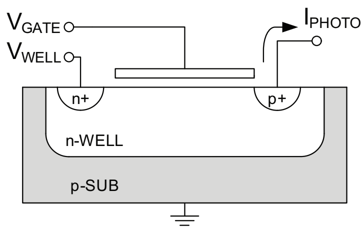

Fig. 2: Spectrally-sensitive photodiode (SPD) inspired by [6], modified for a p-type substrate.

where ϕ is the radiation intensity, q is the elementary charge, S is the area of the sensor, λ is the wavelength, h is Planck's constant, c is the speed of light in vacuum, α is the absorption coefficient, and ω is the absorption depth.

To sense colored light, the SPD inspired by [6], [7] depicted in Fig. 2, applies a voltage V_{GATE} to a poly-silicon gate to modulate the depth of the photo sensing region beneath the gate, which corresponds to modulating ω. The poly-silicon gate attenuates light (e.g., at 600nm by approximately 50% [9]), which can be improved by optimizing the gate material [10]. Only photo-induced electrons generated at a depth shallower than ω are collected to form a photocurrent. Thus, controlling ω via the gate voltage enables spectral sensitively.

When two different wavelengths are incident simultaneously, the currents generated at the absorption depths of ω_1 and ω_2 are expressed respectively as

$$I_1 = \frac{\phi_1 q S \lambda_1}{hc}(1 - e^{-\alpha_1 \omega_1}) + \frac{\phi_2 q S \lambda_2}{hc}(1 - e^{-\alpha_2 \omega_1}) \quad (2)$$

$$I_2 = \frac{\phi_1 q S \lambda_1}{hc}(1 - e^{-\alpha_1 \omega_2}) + \frac{\phi_2 q S \lambda_2}{hc}(1 - e^{-\alpha_2 \omega_2}) \quad (3)$$

where ϕ_1 and ϕ_2 are the intensities with wavelengths λ_1 and λ_2, respectively, and absorption coefficients α_1 and α_2, respectively. The absorption depths ω_1 and ω_2 are modulated by the gate voltage of the SPD. Both illumination intensities (ϕ_1, ϕ_2) can be found by solving these simultaneous equations, involving two measurements of the currents (I_1, I_2) over two different depths (ω_1, ω_2).

III. Standard-CMOS Field-Modulated Color Sensors

In order to explore the utility of the field-modulated color sensor in [6], [7] in a standard CMOS technology, an investigation has been conducted by us using a 0.35μm process prototype with a SPD structure depicted in Fig. 2. As CMOS technology scales, the SPD photo response may deviate from the above physical model. Equations (2) and (3) take the form of (4) and (5), respectively

$$I_1 = k_{11}\phi_1 + k_{12}\phi_2 \quad (4)$$

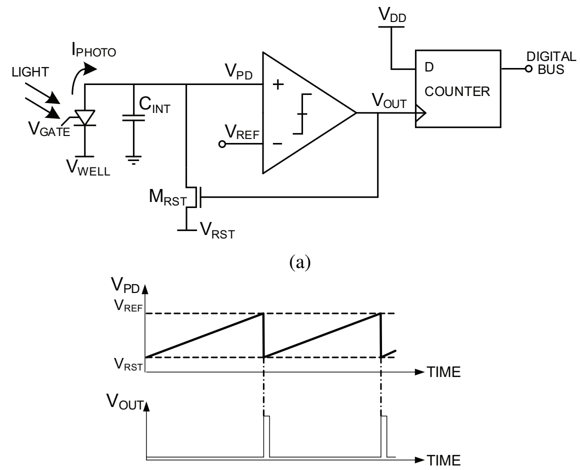

Fig. 3: FCS implementation. (a) FCS circuit with current-to-frequency ADC. (b) Voltage transients under illumination.

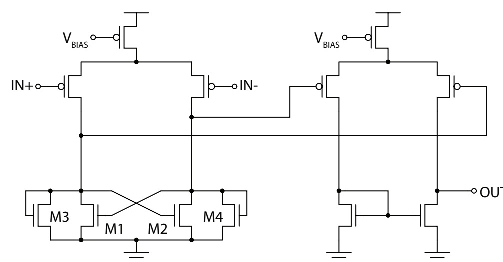

Fig. 4: The voltage comparator.

$$I_2 = k_{21}\phi_1 + k_{22}\phi_2 \quad (5)$$

where the k-parameters describe the transfer function of the SPD and can be obtained empirically. This model can be extended to a finite set of N wavelengths. To determine the intensity of an input spectrum to a resolution of N distinct wavelengths, N measurements are required across N detection depths. Equations (4) and (5) thus extend to the N-equation matrix

$$\begin{bmatrix} I_1 \\ I_2 \\ \vdots \\ I_N \end{bmatrix} = \begin{bmatrix} k_{11} & k_{12} & \cdots & k_{1N} \\ k_{21} & k_{22} & \cdots & k_{2N} \\ \vdots & \vdots & \ddots & \vdots \\ k_{N1} & k_{N2} & \cdots & k_{NN} \end{bmatrix} \begin{bmatrix} \phi_1 \\ \phi_2 \\ \vdots \\ \phi_N \end{bmatrix} \quad (6)$$

To construct a $N \times N$ k-matrix model in (6) of a SPD empirically, it is illuminated by light of known intensities at N wavelengths and the corresponding currents are measured. The model is then used to compute unknown light intensities at the same wavelengths based on measured currents $\boldsymbol{I}$ by solving the system of equations (6) for $\boldsymbol{\phi}$.

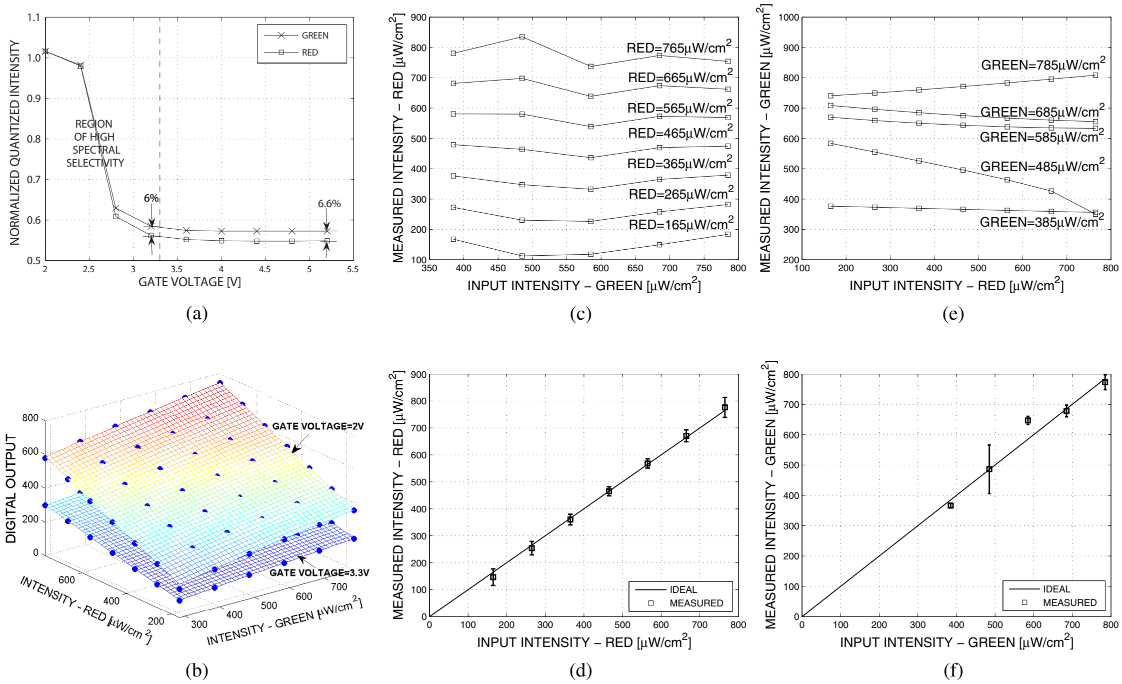

Fig. 5: Experimental results. (a) Measured photo response of the FCS normalized at V_{GATE} = 2V. (b) Measured photo responses of the FCS across gate voltages and illumination. (c) Measured intensity at discrete red (640nm) levels across green (540nm) levels. (d) Measured vs. input intensity at 640nm. (e) Measured intensity at discrete green levels across red levels. (f) Measured vs. input intensity at 540nm.

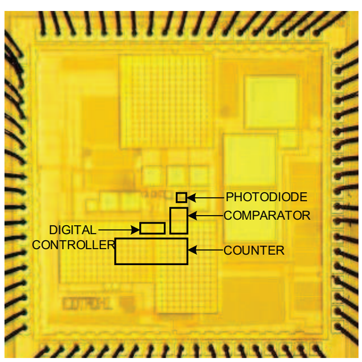

Fig. 6: Chip micrograph of the field-modulated color sensor.

IV. VLSI Implementation

The overall FCS circuit is depicted in Fig. 3(a). The FCS converts the photocurrent generated by the SPD to a 16-bit digital output, which is then fed into a reconstruction software that solves for the input spectrum ϕ in (6). The FCS is implemented using a current-to-frequency ADC architecture [4] that measures the light intensity by counting the number of resets during the integration time. It is insensitive to supply voltage scaling as it removes the voltage headroom constraint by representing light intensity in the temporal domain. In the beginning of each integration period, the counter is cleared and the photodiode output V_{PD} is precharged to the reset voltage V_{RST} = 0V. The n-well is biased at the voltage V_{WELL} = 2.4V. The photocurrent causes V_{PD} to rise, charging the integration capacitor C_{INT}, whose value can be optimized for the illumination dynamic range. When V_{PD} reaches the comparator reference voltage V_{REF} = 1.5V, the comparator changes state, causing the reset transistor M_{RST} to turn on, resetting V_{PD} to V_{RST}. After reset, the comparator output toggles back to the original state. The resultant pulse train, as depicted in Fig. 3(b), has a pulse frequency proportional to incident light intensity.

Fig. 4 depicts the comparator schematic. It is a two-stage design with PMOS input transistors to minimize the flicker noise. The first stage employs cross-coupling to increase the output resistance of the load transistors M_1 through M_4. The second stage provides an additional gain. The first stage and the second stage consume 18μA and 10μA, respectively.

V. Measurement Results

Fig. 6 depicts the micrograph of the prototype implemented in a 0.35μm standard CMOS technology. It has been tested in light intensity measurements at the red (640nm) and green (540nm) wavelengths. Two current-controlled light-emitting diodes (LEDs) provide input illumination. The photo response of the

TABLE I: EXPERIMENTAL CHARACTERISTICS

Technology	0.35μm CMOS
Supply Voltage	3.3V
Power Consumption	0.3mW
Pixel Size	50μm x 50μm
Core Area	0.5mm$\times$0.5mm
Integration Capacitance	1pF
Counter Size	16-bit
Optical Sensitivity	1μW/cm^2/level
Dark Current	0.25 count/sec
Max. Pulse Frequency	10MHz

fabricated SPD is first characterized to determine the optimal gate voltages for field modulation. Fig. 5(a) depicts the measured photo response of the FCS across gate voltages for red and green light. For V_{GATE} from 2V to 5.2V, the change in the photocurrent due to red illumination is 6.6% less than that due to green illumination. The FCS spectral selectivity is based on this difference and is most prominent between the V_{GATE} of 2V to 3.3V. For FCS operation within the nominal supply voltage, V_{GATE} of 2V and 3.3V are chosen for two modulation settings.

In order to build an empirical model for the FCS to measure the intensity at two known wavelengths λ_1=540nm and λ_2=640nm, the SPD is characterized by simultaneously shining different combinations of input intensities at λ_1 and λ_2. For each input combination, the photocurrent is measured using the chosen discrete gate voltages. Fig. 5(b) depicts the measured SPD response for the gate voltages of 2V and 3.3V. It is worth noting that (4) and (5) require only one red and one green known light intensity to determine all four k-parameters. But it has been found that modeling accuracy can be improved by simultaneously utilizing multiple combinations of red and green light intensities to solve for the average k-parameters. Therefore, each of the two planes is utilized to find the average k-parameters in equations (4) and (5), respectively.

Fig. 5(c) depicts measured intensities for an illumination that simultaneously contain light power at 640nm and 540nm, computed using equations (4) and (5). It shows the intensity for discrete red input levels across different green inputs. Measurement of an input at a particular wavelength should ideally be insensitive to a change in the light intensity at the other input wavelengths and therefore the plot should ideally be a family of horizontal lines. Fig. 5(d) is plotted as an alternative for visualizing the data of Fig. 5(c) with respect to the intensity of red light. It depicts measured red intensity, with each data point containing a sweep across different green intensities. The error bars depict one standard deviation away from the mean value.

Fig. 5(e) and (f) are similar to Fig. 5(c) and (d), respectively, but for the green wavelength. A low green intensity of 285μW/cm^2 have also been utilized in the tests but has yielded wide variation between measurements. The generally larger error observed in the green measurements may be due to several effects. At the depth where green light is present, red light is also present. But the converse is not true to the same extent. Due to this physical property, sensing at longer wavelengths may in general be more accurate. Also, as measured by an optical power meter, the green LED exhibits less linearity in respect to the input current than the red LED, especially in the extremes of the range utilized in the tests. Nonetheless, Figs. 5(c) through (f) demonstrate intensity measurements that validate color sensitivity of the FCS at two wavelengths 100nm apart. A summary of the experimental characteristics is provided in Table I.

VI. Conclusion

We have demonstrated a digital color sensor that senses wavelengths 100nm apart implemented solely using structures available in a standard CMOS technology. A color-sensitive photodiode and a current-to-frequency ADC have been fabricated on the same CMOS die. High level of integration, reduced power consumption, and simplified optics are features that enable ubiquitous low-cost multi-color fluorescent imaging.

References

[1] H. Ai, K. Hazelwood, M. Davidson, and R. Campbell, "Fluorescent protein FRET pairs for ratiometric imaging of dual biosensors," *Nature Methods*, vol. 5, no. 5, pp. 401–403, 2008.

[2] X. Gao, Y. Cui, R. Levenson, L. Chung, and S. Nie, "In vivo cancer targeting and imaging with semiconductor quantum dots," *Nature Biotechnology*, vol. 22, no. 8, pp. 970–976, 2004.

[3] S. Kong, D. Wijngaards, and R. Wolffenbuttel, "Infrared microspectrometer based on a diffraction grating," *Sensors and Actuators A*, no. 92, pp. 88–95, 2001.

[4] J. Correia, G. Graaf, M. Bartek, and R. Wolffenbuttel, "A single-chip CMOS optical microspectrometer with light-to-frequency converter and bus interface," *IEEE J. Solid-State Circuits*, vol. 37, no. 10, pp. 1344–1347, Oct 2002.

[5] X. Fang, V. Hsiao, V. Chodavarapu, A. Titus, and A. Cartwright, "Colorimetric porous photonic bandgap sensors with integrated CMOS color detectors," *IEEE Sensors Journal*, vol. 6, no. 3, pp. 661–667, Jun 2006.

[6] Y. Maruyama, K. Sawada, H. Takao, and M. Ishida, "A novel filterless fluorescence detection sensor for DNA analysis," *IEEE Trans. Electron Devices*, vol. 53, no. 3, pp. 553–558, Mar 2006.

[7] H. Ishii, Y. Maruyama, H. Takao, M. Ishida, and K. Sawada, "Improvement in filter-less fluorescence sensor capability by optimization of potential distribution," *4th Asia-Pacific Conf. on Transducers and Micro-Nano Tech.*, pp. 68–71, Jun 2008.

[8] J. Mckelvey, *Solid State and Semiconductor Physics*. New York: Harper and Row, 1966.

[9] H. Wong, "Technology and device scaling considerations for CMOS imagers," *IEEE Trans. on Electron Devices*, vol. 43, no. 12, pp. 2131–2142, Dec 1996.

[10] J. Halvis, N. Bluzer, R. Shiskowski, and L. Chen, "Method of making transparent polysilicon gate for imaging arrays," *Patent No. 5369040*, Nov 1994.